PNAS Nexus, 2023, 2, 1–14
https://doi.org/10.1093/pnasnexus/pgad251
Advance access publication 22 August 2023
Research Report

Transient anxiety-and depression-like behaviors are linked to the depletion of Foxp3-expressing cells via inflammasome in the brain

Eun-Jeong Yang[a], Md Al Rahim[a], Elizabeth Griggs[a], Ruth Iban-Arias[a] and Giulio Maria Pasinetti[a,b,*]

[a]Department of Neurology, Icahn School of Medicine at Mount Sinai, New York, NY 10029, USA
[b]Geriatric Research, Education and Clinical Center, James J. Peters Veterans Affairs Medical Center, Bronx, NY 10468, USA
*To whom correspondence should be addressed: Email: giulio.pasinetti@mssm.edu
Edited By: Andrey Abramov

Abstract

Forkhead box P3 (Foxp3) is a transcription factor that influences functioning of regulatory T cells (Tregs) that modulate peripheral immune response. Treg-mediated innate immunity and Treg-mediated adaptive immunity are receiving considerable attention for their implication in mechanisms associated with anxiety and depression. Here, we demonstrated that depletion of Foxp3-expressing cells causally promotes transient anxiety- and depression-like behaviors associated with inflammasome activation in "depletion of regulatory T cell" (DEREG) mice. We found that restoration of Foxp3-expressing cells causally reverses neurobehavioral changes through alteration of innate immune responses as assessed by caspase-1 activity and interleukin-1β (IL-1β) release in the hippocampal formation of DEREG mice. Moreover, we found that depletion of Foxp3-expressing cells induces a significant elevation of granulocytes, monocytes, and macrophages in the blood, which are associated with transient expression of the matrix metalloprotease-9. Similarly, we found that depletion of Foxp3-expressing cells in 5xFAD, a mouse model of Alzheimer's disease (AD), exhibits elevated activated caspase-1 and promotion of IL-1β secretion and increased the level of amyloid-beta $(Aβ)_{1–42}$ and Aβ plaque burden in the hippocampal formation that coincided with an acceleration of cognitive decline at a presymptomatic age in the 5xFAD mice. Thus, our study provides evidence supporting the idea that Foxp3 may have a causal influence on peripheral immune responses. This, in turn, can promote an innate immune response within the brain, potentially leading to anxiety- and depression-like behaviors or cognitive decline.

Keywords: Foxp3, inflammasome activation, depression, anxiety, transient

Significance Statement

In this study, we elucidate the potential role of forkhead box P3 (Foxp3), a transcription factor of regulatory T cells, in mechanisms associated with neurobehavioral changes including anxiety- and depression-like behaviors using Foxp3 conditional knockout mice. We found that dynamic regulation of Foxp3-mediated inflammatory responses may be causally associated with anxiety- and depression-like behaviors through transient promotion and reversal of innate immunity in the brain. Our study includes interesting results regarding a potential mechanism for therapeutic intervention in anxiety and depression by targeting innate immunity in the brain through modulation of the expression of the Foxp3 transcription factor in regulatory T cells.

Introduction

Anxiety and depression are common and highly prevalent neuropsychiatric symptoms across many neurological disorders (1). Clinical and preclinical studies provide extensive evidence indicating that anxiety and depression are linked to changes in neuroplasticity within corticolimbic brain regions, including neuronal atrophy and synapse loss (2, 3). The dysregulation of neuroimmune systems, mediated by microglia, contributes to the development and manifestation of anxiety and depression in neurological disorders, coinciding with the observed alterations in neuroplasticity (4–8). While it has been established that microglia play a significant role in anxiety and depression, the causal mechanisms that underlie their contribution to the development of these conditions are still under investigation.

The brain is considered an immune-privileged organ; however, several studies recently revealed that immune responses in the brain are influenced by peripheral immunity (9). Peripheral inflammatory cascades increase permeability of the blood–brain barrier (BBB) through mechanisms involving the disruption of endothelial tight junctions or increased expression of matrix metalloproteinases (MMPs) such as MMP-9 (10, 11), leading to

Competing Interest: The authors declare no competing interest.
Received: April 25, 2023. **Revised:** July 17, 2023. **Accepted:** July 20, 2023

permeation of proinflammatory mediators into the brain (12). However, the pathophysiological features of these cascades and their association with permanent or transient damages influencing neurobehavioral responses are also unknown. Thus, it is imperative to investigate whether activation of peripheral immunity may causally promote transient or permanent pathophysiological conditions in the brain for the design of novel prevention interventions in mood and cognitive disorders.

The transcription factor, forkhead box P3 (Foxp3), plays a major role in the differentiation and activation of regulatory T cells (Tregs) (13). Tregs are required for maintenance of immunological self-tolerance and immune homeostasis (14). For example, a missense mutation in the *Foxp3* gene or depletion of Foxp3 expression impairs development and maintenance of Treg function, leading to regulation of innate and adaptive immunity (15, 16). Eventually, impairments of Tregs lead to their inability to suppress inflammation in the peripheral immune system and causes autoimmune disorders including rheumatoid arthritis, systemic lupus erythematosus, and multiple sclerosis (17).

Recently, Tregs have received significant attention for their potential role in the development of anxiety and depression (8). Evidence suggests that decreased Foxp3 expression is associated with major depressive disorders (MDD) (18) and is correlated with inflammatory conditions characterized by increased levels of circulating proinflammatory cytokines (19). Additionally, epigenetic regulation of *Foxp3* promoter is associated with loss of Treg function in anxiety (20). Interestingly, recent studies suggest efficacy of antidepressant or anxiolytic drugs through mechanisms influencing Foxp3 expression and the regulation of Treg-associated cytokines such as interleukin (IL)-2, IL-10, and transforming growth factor-β (21). Thus, it is possible that Foxp3 may influence anxiety and depression through mechanisms involving regulation of the peripheral immune system.

Based on this, the present study investigated the casual role of Foxp3-expressing cells in the promotion of neurobehavioral responses associated with neuroimmune cross-talking between the peripheral and central immune systems. Using a "depletion of regulatory T cell" (DEREG) mouse expressing a diphtheria toxin receptor (DTR)–enhanced green fluorescent protein (GFP) transgene controlled by a *Foxp3* promoter, we found that transient depletion of Foxp3-expressing cells causally promoted transient anxiety- and depression-like behaviors possibly through mechanisms involving transient activation of inflammasomes, MMP-9 expression in the brains, and dysregulation of circulating innate immune cells. We also found that depletion of Foxp3-expressing cells in 5x familial Alzheimer disease (5xFAD) mice, a mouse model of Alzheimer's disease (AD), is casually associated with AD-type cognitive impairments and neuropathological changes. This study suggests a causative role of Treg depletion in the proliferation of peripheral immune cells that concomitantly contributes to transient activation of innate immunity in the brain and causing anxiety, depression, or impaired cognitive function.

Materials and methods

Animals

All of the experimental procedures were approved by the Mount Sinai Institutional Animal Care and Use Committee (IACUC) (Approval number: IPROTO202100000013). DEREG mice expressing a DTR-enhanced GFP transgene controlled by a *Foxp3* promoter were purchased from Jackson Laboratories (strain: C57BL/6-Tg [Foxp3-DTR/EGFP]23.2Spar/Mmjax) and maintained by crossing C57BL/6J mice. Transgenic offspring were genotyped by PCR using the primers (forward, F, 5′-CCCAGGTTACCATG GAGAGA-3; reverse, R, 5′-GAACTTCAGGGTCAGCTTGC-3′) and nontransgenic littermates served as age-matched control. Double transgenic mice were generated by cross-breeding with DEREG mice and 5xFAD mice that were purchased from Jackson Laboratories (strain: B6SJL-Tg [APPSwFlLon, PS1*M146L*L286V] 6799Vas/J). Double transgenic mice were identified by PCR, and nontransgenic littermates served as age-matched controls. Heterozygous of DEREG or double heterozygous of 5xFAD/DEREG mice were utilized for all experiments. The number of mice used for each experiment is indicated in the figure legends, ranging from 5 to 15. All mice were housed on a 12-h light/dark cycle in a temperature-controlled environment.

Administration of diphtheria toxin

In order to set a protocol for administration of diphtheria toxin (DT) (D0564; Sigma, MO, USA), DEREG mice were treated with 100 and 300 ng of DT or phosphate-buffered saline (PBS) to deplete Foxp3-expressing cells without nonspecific effects. This experiment was performed independently. For other experiments, 2-month-old DEREG mice were i.p. injected every 4 days for 6 weeks with 300 ng of DT or PBS (Fig. 1B). Double transgenic mice, 2-month-old 5xFAD/DEREG mice, were treated every 4 days for 15 weeks with 300 ng of DT or PBS (Fig. 6).

Behavioral tests

Behavioral tests were performed with a near-infrared camera and measured with ANY-maze tracking software (Stoelting, IL, USA). All animals were handled for 10 min per day for 5 days prior to experiments and were habituated to the testing room for 1 h at the beginning of the test day. All behavioral paradigms were carried out according to established protocols and described briefly below:

1. Open field (OF) test: To measure total distance traveled for locomotion activity, each mouse was placed in a white box (42.5 cm $L \times 42.5$ cm $W \times 42.5$ cm H) and was recorded for 10 min. Total distance traveled was calculated by ANY maze software.
2. Light and dark box (LD) test: To assess anxiety-like behavior, each mouse was placed in light–dark box (each compartment; 20 cm $L \times 40$ cm $W \times 40$ cm H) and allowed to explore the box freely. Each test was recorded for 10 min with a camera attached to the ceiling. Time spent inside the dark compartment was calculated by an automated video-tracking system (ANY-maze software)
3. Forced swimming test (FST): To assess depressive-like behavior, mice were put in a transparent plastic cylinder (45 cm high and 20 cm in diameter) filled with water, and each test was recorded with a digital camera for 6 min. The total duration of immobility, defined as the absence of movement in all four limbs, was measured using ANY-maze software.
4. Novel object recognition (NOR) test: NOR was conducted to assess cognitive function as described in previous research with minor modifications (22). During habituation, mice were placed in a white box for 10 min. The next day, mice were placed in a white box with two similar objects and were allowed to interact with the objects for 10 min. After 10 min of training, one object was replaced with a novel object, and mice were placed in the box to interact with objects for 10 min. To measure cognitive function, discrimination index was analyzed using ANY-maze software and was calculated as $\text{Time}_{\text{novel}}/(\text{Time}_{\text{novel}} + \text{Time}_{\text{familiar}}) \times 100$.

Cells or tissue preparation

Single-cell suspension samples processed for flow cytometry and cytometry by time of flight (CyTOF) were derived from mouse blood collected by retroorbital bleeding. Each blood sample was placed in a tube with ethylenediaminetetraacetic acid, and peripheral blood mononuclear cells (PBMC) were extracted by serially lysing red blood cells (RBC) in an RBC lysis buffer (00-4300-54; Invitrogen, MA, USA). For tissue (spleen and brain) collection, mice from all groups were perfused after performing behavior tests. The brain tissues were separated into two hemispheres equally. One hemisphere was further dissected into the hippocampal formation, and the other hemisphere was fixed with 4% paraformaldehyde for 24 h. All samples were stored at −80°C or 4°C before further analysis.

Flow cytometry

Cell surface and intracellular staining were performed with monoclonal antibodies against CD3e (56-0032-82, Thermo Fisher Scientific, MA, USA) and CD4 (56-0032-82, Thermo Fisher Scientific). For intracellular staining, Foxp3 fixation/permeabilization kit (00-5523-00, Thermo Fisher Scientific) was used according to the manufacturer's instructions. Fluorescence intensities were examined as assessed by Attune NxT (Thermo Fisher Scientific) flow cytometer at the Icahn School of Medicine flow cytometry core, and data were analyzed using FCS express software (CA, USA).

RNA sequencing, library preparation, and analysis

Total RNA was extracted using Qiagen RNeasy Plus Mini kit (74134, Qiagen, Hilden, Germany). The RNA sequencing library was prepared using the NEBNext Ultra II RNA Library Prep Kit for Illumina (New England Biolabs, MA, USA). Samples were sequenced using a 2 × 150 bp paired-end configuration. After investigating the quality of the raw data, sequence reads were trimmed to remove possible adapter sequences and nucleotides with poor quality. The trimmed reads were mapped to the *Mus musculus* reference genome available on ENSEMBL. Unique gene hit counts that fell within exon regions were calculated by using feature counts from the subread package. After extraction of gene hit counts, the gene hit count table was used for downstream differential expression analysis. Using DESeq2, a comparison of gene expression between the groups of samples was performed. The Wald test was used to generate *P* values and $\log_2$ fold changes. Significantly differentially expressed genes (DEGs) were defined by *P* values less than 0.05. For the canonical pathways, diseases/bio functions, and molecular networks analysis of DEGs, we used the commercial QIAGEN Ingenuity Pathway Analysis (IPA, QIAGEN) software. For the canonical pathways, diseases/bio functions, and comparison analysis, −log (*P* value) > 1.3 was taken as the threshold, a Z score > 2 was defined as the threshold of activation, and a Z score < −2 was defined as the threshold of inhibition. The score of molecular network analysis was calculated by IPA.

Western blotting

Extracted protein samples from hippocampal formation (45 μg) were separated by electrophoresis on 4 to 15% sodium dodecyl sulfate–polyacrylamide gels and transferred to a nitrocellulose membrane. The membranes were then blocked for 1 h at room temperature (RT), followed by overnight treatment with primary antibodies (anti-caspase-1 antibody, 20B-0042; anti-IL-1β antibody 6243S; anti-α-tubulin antibody, T9026) at 4°C. The next day, the blots were treated with a secondary antibody conjugated with horseradish peroxidase (anti-rabbit or anti-mouse IgG-HRP antibodies) for 1 h at RT. The bands were detected using chemiluminescence detection kit (32106; Thermo Fisher Scientific). The blots were treated with a stripping buffer consisting of β-mercaptoethanol, sodium dodecyl-sulfate, and Tris–HCl (Biorad, CA, USA). Subsequently, the stripped blots were probed again, enabling the identification and detection of distinct proteins with similar molecular weights on the same blot. Data were analyzed using ImageJ software to measure relative protein expression.

RNA extraction and qRT-PCR

Total RNA from the brain, spleen, and PBMC were extracted using Quick RNA extraction Kit (Zymo research, CA, USA). Strand cDNA was synthesized from 100 ng of total RNA using High-Capacity cDNA Reverse Transcription Kit (4368814, Applied Biosystems, MA, USA) as per the manufacturer's instructions. qRT-PCR was performed by the Icahn School of Medicine qPCR Core and analyzed by ABI PRISM 7900HT Sequence Detection System (Applied Biosystems). Utilized cycling conditions were as follows: 95°C for 2 min, followed by 40 cycles of 95°C for 15 s, 60°C for 15 s, and 72°C for 1 min. The primer sequences were as follows: *Foxp3*-F, 5′-AGAGCTCTTGTCCATTGAGGCCA-3′, *Foxp3*-R, 5′-TGTCCTGGG CTACCCTACTG-3′; *Cxcl10*-F, 5′-ATGACGGGCCAGTGAGAATG-3′, *Cxcl10*-R, 5′-GAGGCTCTCTGCTGTCCATC-3′; *Caspase-1*-F, 5′-CA CATTTCCAGGACTGACTGG-3′, *Caspase-1*-R, 5′-AGACGTGTACGA GTGGTTGT-3′; *Nlrp3-F*, 5′-AGAAGAGACCACGGCAGAA-3′, *Nlrp* 3-R, 5′-CCTTGGACCAGGTTCAGTGT-3′; *IL-1β*-F, 5′-TTCAGGCA GGCAGTATCACTC-3′; *IL-1β*-R, 5′-CCACGGGAAAGACACAGGTAG-3′; and *Hprt-F*, 5′-CCCCAAAATGGTTAAGGTTGC-3′, *Hprt-R*-5′-AACAAA GTCTGGCCTGTATCC-3. Expression level of *Hprt* was used as an internal control, and relative mRNA expression of other genes were quantified using the $2^{-\Delta\Delta Cq}$ method.

CyTOF and data analysis

All samples were processed by the Mount Sinai Human Immune Monitoring Center, and CyTOF was conducted as described in previous research (23). Normalized data files were analyzed using the FCS express software for manual cleaning and gating different immune cells to create 2 and high-dimensional (t-distributed stochastic neighbor embedding [t-SNE]) plots. t-SNE clustering was performed on 16 parameters where equal event sampling was selected in PBMC. t-SNE analysis was performed using equal sampling per comparison, perplexity = 80 and iterations = 1,000.

Cytokine array

Proteome Profiler Array (ARY006; R&D System, MN, USA) was used to measure cytokines, chemokines, and acute phase protein as described previously (24). Briefly, 100 μl of plasma samples in blocking buffer were incubated to membranes containing antibody arrays overnight as at 4°C on a shaker. The membranes were incubated with the biotinylated antibody cocktail solution and horseradish peroxidase–conjugated streptavidin for 3 or 2 h at RT, respectively. All membranes were developed with the detection reagent provided by the manufacturer and were scanned to obtain images for analysis of pixel densities using the ImageJ software. Positive controls were used for normalization, and mean values were calculated.

Enzyme-linked immunosorbent assays

Enzyme-linked immunosorbent assays (ELISAs) were performed using mouse amyloid beta$_{1–40}$ (A$\beta_{1–40}$, KMB3481; Invitrogen) and mouse A$\beta_{1–42}$ (KMB3441; Invitrogen) ELISA kits to determine the amount of A$\beta_{1–40}$ and A$\beta_{1–42}$ following the manufacturer's

instructions. Briefly, frozen brain tissues were homogenized in a cold buffer, which consisted of 5 M guanidine–HCl/50 mM Tris supplemented with inhibitor cocktail containing AEBSF (78431; Thermo Fisher Scientific) and then incubated with an orbital shaker for 3 h at RT. A total of 100 µl of standards and sample, which were diluted with standard diluent buffer, were applied to $A\beta_{1-40}$ or $A\beta_{1-42}$ polyclonal antibody–precoated 96-well plates. The plates were read at 450 nm using a microplate reader (VarioskanTM Lux; Thermo Fisher Scientific). Concentrations of $A\beta_{1-40}$ and $A\beta_{1-42}$ were calculated using the standard curves, and both were normalized by total amount of protein from each sample using the BCA assay (23225; Thermo Fisher Scientific).

Immunohistochemistry

Brains were cut into 50-µm coronal sections, and sections were washed in PBS and incubated in blocking solution (10% normal goat serum, 0.1% Triton X-100) for 1 h at RT. Sections were then incubated with primary antibody in blocking solution overnight at 4°C. 6E10 (SIG39320, Biolegend, CA, USA) was used as a primary antibody. After the primary immunoreaction, sections were incubated with Alexa 488 (A11001, Invitrogen) conjugated secondary antibodies. LSM 800 confocal microscope (Carl Zeiss, Jena, Germany) was used for visualization of immunostaining of the sections.

Statistical analysis

All data are expressed as the mean ± SEM. Data were calculated using a *t* test, Wald test, one or two-way ANOVA followed by Tukey's post hoc analysis ($^*P < 0.05$, $^{**}P < 0.01$, $^{***}P < 0.001$). All statistical analyses were performed using GraphPad Prism 8 software (GraphPad Software Inc., San Diego, CA, USA).

Results

Dynamical regulation of Foxp3-expressing cells is mediated by DT treatment in DEREG mice

Here, we investigated the regional distribution of mRNA expression of *Foxp3* in the PBMC, spleen, and brain to estimate abundance of Foxp3 expression in DEREG mice. As shown in Fig. 1A,

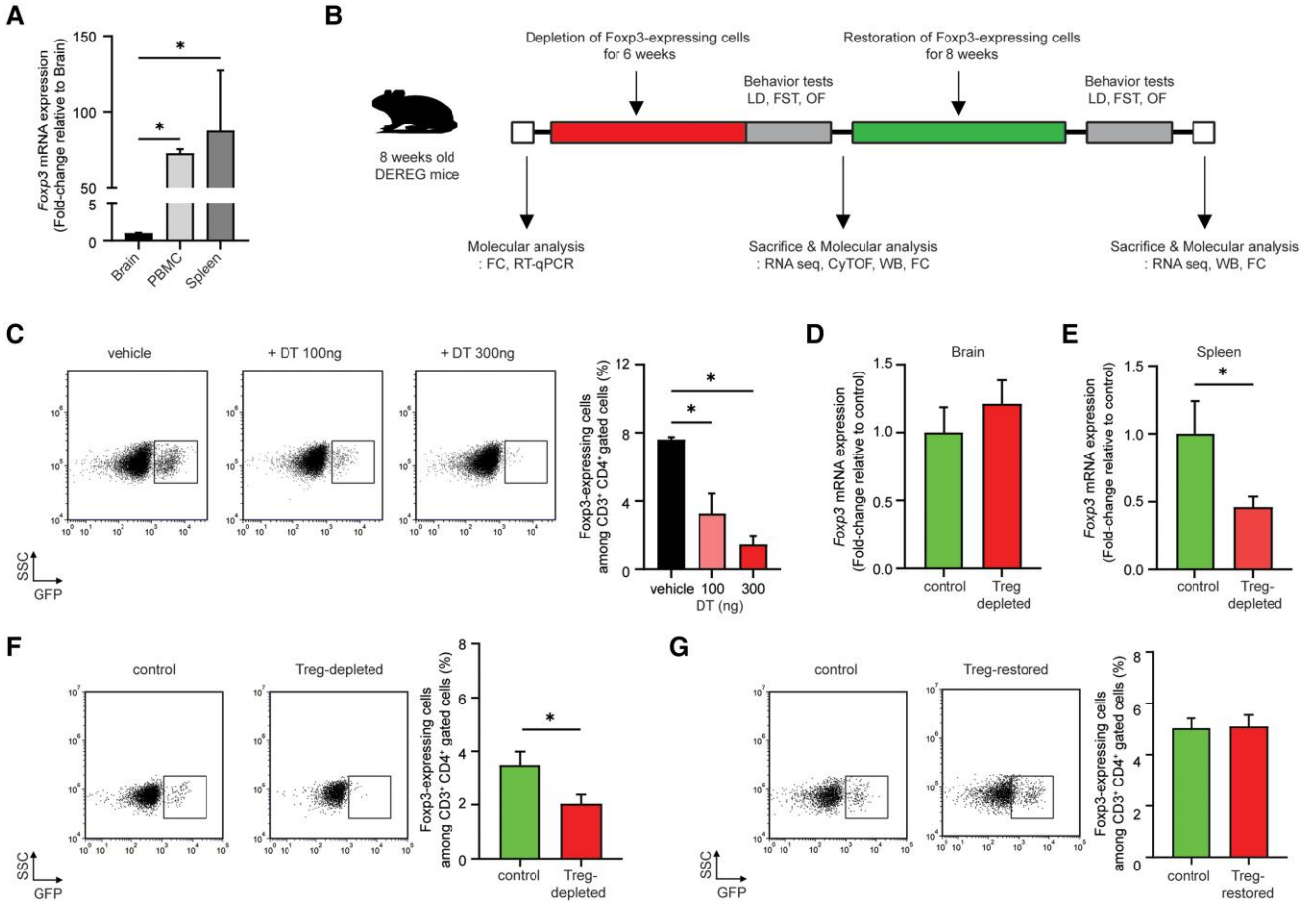

Fig. 1. Transient depletion of Foxp3-expressing cells followed by DT treatment in DEREG mice. A) A bar graph showing *Foxp3* mRNA expression in the brain, PBMC, and spleen. Statistical analyses were performed using one-way ANOVA, followed by Tukey's post hoc analysis ($^*P < 0.05$, compare with *Foxp3* mRNA expression in the brain, $n = 3$–6 mice for each group). B) Experimental outline. FC, flow cytometry; RNA seq, RNA sequencing; CyTOF, cytometry by time of flight; WB, western blot; LD, light and dark box; FST, forced swimming test; OF, open field. C) Representative flow cytometry analysis of GFP expression by gated $CD3^+CD4^+$ cells (left panel). Biexponential scale used for representative flow cytometry. A bar graph showing percentage of Foxp3-expressing cells among $CD3^+CD4^+$ cells in PBMC of DEREG mice followed by treatment of different doses of DT (right panel). Statistical analyses were performed using one-way ANOVA, followed by Tukey's post hoc analysis ($^*P < 0.05$, compare with control group, $n = 3$–4 mice for each group). D, E) *Foxp3* mRNA expression D) in the brain and E) in spleen followed by DT treatment in DEREG mice. Bar graphs showing relative quantification of *Foxp3* mRNA expression in Treg-depleted and age-matched control mice. F, G) Representative flow cytometry analysis of GFP expression by gated $CD3^+CD4^+$ cells from PBMC in F) Treg-depleted mice and in G) Treg-restored mice compared with age-matched control mice. Bar graphs showing percentage of Foxp3-expressing cells among $CD3^+CD4^+$ cells. Biexponential scale used for representative flow cytometry. Statistical analyses were performed using *t* test ($^*P < 0.05$, compared with age-matched control mice, $n = 5$–7 mice for each group). Data are expressed as the means ± SEM.

Foxp3 mRNA expression in PBMC and spleen were approximately two orders of magnitude higher compared with its expression in the brain.

We utilized DEREG mice, expressing DTR-eGFP transgene under control of *Foxp3* promoter, allowing depletion of Foxp3-expressing cells by DT treatment transiently (Fig. 1B). These DT-treated mice (Treg-depleted mice) showed a dose-dependent decrease in Foxp3-expressing cells compared with the vehicle-treated mice, after treatment of DT with different concentrations (100 and 300 ng) for 6 weeks (Fig. 1C). Based on titration of study, we selected the dose of 300 ng of DT to deplete Foxp3-expressing cells for subsequent experiments (Fig. 1B). We next examined whether DT treatment induces depletion of Foxp3-expressing cells in the brain, spleen, and PBMC in Treg-depleted mice (Fig. 1D–F). We found no difference in *Foxp3* mRNA expression in the brain of Treg-depleted mice compared with age-matched control mice (Fig. 1D). However, *Foxp3* mRNA expression was significantly decreased by 46% in the spleen of Treg-depleted mice compared with age-matched control (Fig. 1E).

We also observed that Foxp3-expressing cells were significantly reduced by approximately 60% in PBMC of Treg-depleted mice (Fig. 1F). Moreover, reduction of Foxp3-expressing cells in PBMC returned to baseline level in Treg-restored mice following withdrawal of DT for 8 weeks as assessed by flow cytometry (Fig. 1G).

Taken together, these results indicate that administration of DT in DEREG mice induced transient depletion of Foxp3-expressing cells selectively in PBMC after treatment with 300 ng of DT for 6 weeks, and its expression was restored to the baseline level following withdrawal of DT.

Transient depletion of Foxp3-expressing cells in PBMC is causally associated with the promotion of anxiety- or depression-like behaviors in DEREG mice

To investigate causal association between peripheral Foxp3 expression and anxiety-/depression-like behaviors in DEREG mice, we performed LD, FST, and OF to assess anxiety-like behavior, depression-like behavior, and locomotion activity, respectively. No significant change was observed in body weight between treatment with DT and vehicle in DEREG mice for the treatment period (Figs. 1B and 2A). Changes in locomotor activity after depletion or restoration of Foxp3-expressing cells in DEREG mice were assessed by total distance traveled; no change between Treg-depleted, Treg-restored mice, and age-matched control mice was found (Fig. 2D). These control studies suggest that DT-mediated depletion of Foxp3-expressing cells for 6 weeks was well tolerated in DEREG mice at 300 ng regimen.

In the LD, Treg-depleted mice spent significantly more time in the dark area after depletion of Foxp3 -expressing cells (Fig. 2B, left panel). In addition, we also observed that Treg-depleted mice also exhibited increased immobility time in FST after depletion of Foxp3-expressing cells (Fig. 2C, left panel). Interestingly, these neurobehavioral impairments were ameliorated after restoration of Foxp3-expressing cells in Treg-restored mice compared with age-matched control mice (Fig. 2B and C, right panels). In particular, we found that Foxp3-expressing cells in PBMC were negatively correlated with anxiety- (Fig. 2E) and depression-like behaviors (Fig. 2F).

These results support that transient depletion of Foxp3-expressing cells in PBMC may casually influence anxiety- or depression-like behaviors.

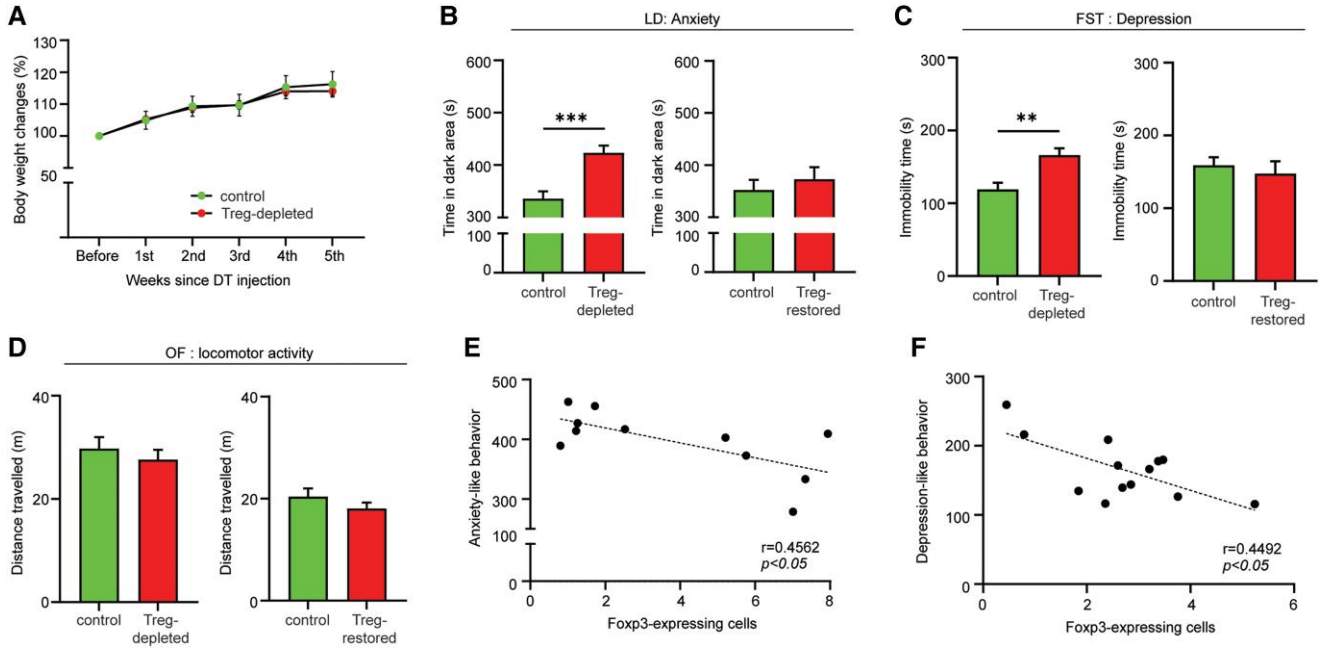

Fig. 2. Transient depression- and anxiety-like behaviors mediated by depletion of Foxp3-expressing cells in DEREG mice. A) Body weight changes in DEREG mice followed by vehicle or DT treatment. B) Bar graphs showing time spent in the dark compartment in Treg-depleted and Treg-restored mice compared with age-matched control mice as a measure of anxiety-like behavior in LD. C) Bar graphs showing total immobility time compartment in Treg-depleted and Treg-restored mice compared with age-matched control mice as a measure of depression-like behavior in FST. D) Bar graphs showing total distance traveled throughout the apparatus compartment in Treg-depleted and Treg-restored mice compared with age-matched control mice as measure of locomotion activity in OF. E, F) Scatter plots representing the correlation between Foxp3-expressing cells and E) anxiety-like behavior and F) depression-like behavior in Treg-depleted and Treg-restored mice. Statistical analyses were performed using *t* test (**$P < 0.01$, ***$P < 0.001$, compared with age-matched control mice, $n = 10$–15 mice for each group). Data are expressed as the means ± SEM.

Transient depletion of Foxp3-expressing cells is causally associated with DEGs related to inflammatory response and immune cell trafficking in the hippocampal formation of Treg-depleted mice

To understand a potential molecular mechanism of the association between peripheral Foxp3-expressing cells and neurobehavioral changes, RNA sequencing was performed in the hippocampal formation of Treg-depleted and Treg-restored mice. Hippocampal formation is one of the crucial brain regions strongly involved in anxiety- and depression-like behaviors in rodents (2).

As shown in Fig. 3A, a total of 17,237 gene DEGs were identified in a volcano plot (Fig. 3A, upper panel) and among these genes, 401 DEGs were up-regulated and 422 DEGs were down-regulated significantly in Treg-depleted mice compared with age-matched control mice (Fig. 3A, bottom panel). To explore the involvement of 823 annotated DEGs in canonical pathways and diseases/bio functions, functional prediction analysis was performed according to IPA software (Fig. 3B and C). For canonical pathway analysis, a total of seven enriched canonical pathways were identified by applying absolute *Z* scores greater than 2 and statistical significance. The top three canonical pathways, "Role of hypercytokinemia/hyperchemokinemia in the pathogenesis of influenza," "Role of pattern recognition receptors in recognition of bacteria and viruses," and "Interferon signaling," were identified among seven other canonical pathways (Fig. 3B, left panel). We also found the expression of 13 DEGs in the top three canonical pathways were significantly altered in Treg-depleted mice compared with age-matched control mice (Fig. 3B, right panel). In addition, diseases and bio function analysis, by applying absolute *Z* scores greater than 2 and statistical significance, revealed activation of functional categories related to "Cell-mediated immune response" and "Immune cells trafficking" in Treg-depleted mice (Fig. 3C).

To investigate whether identified canonical pathways and diseases/bio functions in Treg-depleted mice were transiently altered in Treg-restored mice as found in neurobehavioral changes, a comparison analysis was performed by IPA applying absolute *Z* scores greater than 2 and statistical significance (Fig. 3D and E). As shown in Fig. 3D, we found the top nine canonical pathways being enriched in Treg-depleted mice were recovered in Treg-restored mice. Among these nine canonical pathways, five of them are associated with inflammatory response such as "Role of hypercytokinemia/hyperchemokinemia in the pathogenesis of influenza", "Role of pattern recognition receptors in recognition of bacteria and viruses," "Interferon signaling," "Role of OKR in interferon induction and antiviral response," and "Neuroinflammation signaling" (Fig. 3D). Moreover, significant activated cellular functions, which were related to "Innate immune response" and "Immune cells movement," were observed in Treg-depleted mice, and these changes were significantly mitigated in Treg-restored mice (Fig. 3E).

Taken together, our results suggest that transient depletion of Foxp3-expresing cells promotes inflammatory responses such as immune cell trafficking and inflammasome activation in the hippocampal formation that causally coincided with the transient anxiety- and depression-like behaviors.

Transient depletion of Foxp3-expressing cells results in elevated *Cxcl10* expression and inflammasome activation in DEREG mice

In a validation study of the transcriptomic investigation and IPA analysis (Fig. 3), we assessed mRNA expression of four candidate genes, which are associated with inflammatory responses, in the hippocampal formation of Treg-depleted and Treg-restored mice as assessed by qRT-PCR. We found that mRNA expression of *Cxcl10* (Fig. 4A), a chemokine that plays a key role in controlling leukocyte trafficking into the brain, was significantly elevated in the Treg-depleted mice compared with age-matched control mice (Fig. 4A, left panel), while no significant difference in *Cxcl10* mRNA expression was identified in Treg-restored mice compared with age-matched control mice (Fig. 4A, right panel). We also measured mRNA expression of *Nlrp3*, *Caspase-1*, and *IL-1β* to confirm inflammasome activation in the hippocampal formation of Treg-depleted mice and Treg-restored mice (Fig. 4B–D). The levels of *Nlrp3*, *Caspase-1*, and *IL-1β* mRNA were significantly increased 2-, 1.4-, and 1.3-fold in Treg-depleted mice, respectively (Fig. 4B–D, left panels). Interestingly, no differences in Treg-restored mice were found compared with age-matched control mice (Fig. 4B–D, right panels).

In a further confirmatory study, the protein expression of Pro-caspase-1, Caspase-1, and IL-1β and inflammasome activation markers were assessed by gel blot assay (western blotting, Fig. 4E–H). As shown in Fig. 4E, we confirmed that cleaved Caspase-1 expression (Fig. 4E) and IL-1β expression (Fig. 4F) were significantly increased in Treg-depleted mice compared with those of expression in age-matched control mice (Fig. 4E and F). Interestingly, nondetectable changes in Pro-caspase-1, Caspase-1 (Fig. 4G), and IL-1β (Fig. 4H) in the Treg-restored mice compared with the age-matched control mice were observed.

Overall, these results support the hypothesis that transient depletion of Foxp3-expressing cells may casually and transiently influence brain innate immunity changes that coincided with transient anxiety- and depression-like behaviors.

Depletion of Foxp3-expressing cells increases the number of peripheral innate immune cells coincidentally with transient increase of MMP-9 expression in the brain of DEREG mice

Foxp3 is a specific marker of Treg cells influencing immune tolerance through suppression of immune responses (14). Moreover, Treg cells may also promote innate and adaptive immunity (25, 26). We hypothesized that depletion of Foxp3-expressing cells may modulate innate or adaptive immune cell populations in PBMC. Using CyTOF analysis, we assessed the immune profiles of PBMC in Treg-depleted mice compared with age-matched control mice. To visualize clustering of each cell type, t-SNE analysis was performed based on gate strategy (Fig. 5A and C). All CyTOF were preprocessed, and living single immune cells ($CD45^+$) were retained after gating for further analysis (Fig. 5C). Each immune cell coordinates according to their expression of the six measure parameters including CD3e, CD4, CD8, CD11, CD19, and Ly-6G (Fig. 5A and C). As shown in Fig. 5B, we identified five major immune cell populations, including B lymphocytes ($CD3e^-CD19^+$), $CD4^+$ T lymphocytes ($CD3e^+CD4^+$), $CD8^+$ T lymphocytes ($CD3e^+CD8^+$), macrophages/monocytes ($CD3^-CD19^-CD11b^+LY\text{-}6G^-$), and granulocytes ($CD3^-CD19^-CD11b^+LY\text{-}6G^+$) based on the canonical cell markers. The t-SNE analysis revealed that depletion of Foxp3-expressing cells increased the proportion of granulocytes or macrophages/monocytes, while other subtypes of immune cells (B lymphocytes and T lymphocytes) showed a similar pattern in Treg-depleted mice compared with age-matched control (Fig. 5B). Next, we quantified the subpopulation of each immune cell type in Treg-depleted mice compared with age-matched control (Fig. 5D–F). There were no significant

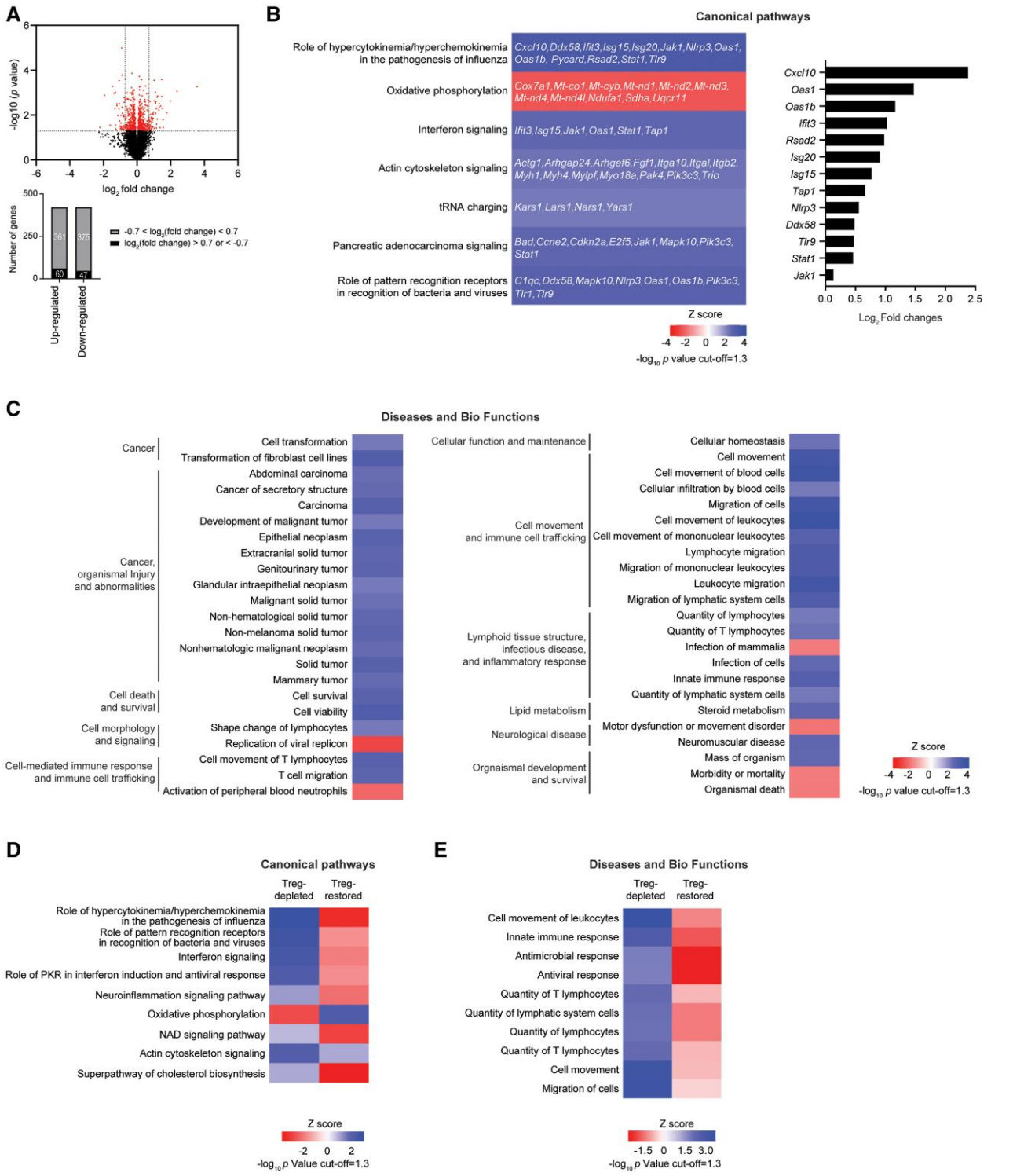

Fig. 3. Alteration of differential gene expression profiles mediated by depletion of Foxp3-expressing cells in hippocampal formation of DEREG mice. A–C) Prediction of biological functions and canonical pathways that are activated or inactivated in Treg-depleted mice compared with age-matched control mice according to IPA analysis. A) A volcano plot (upper panel). The x-axis represents the $\log_2$ conversion of the fold change (FC) values, and the y-axis represents the corrected significance level after base $\log_{10}$ conversion (*P* value). Red dots in the volcano plot indicate all DEGs that were found to differ significantly (*$P < 0.05$). The number of significant DEGs (bottom panel). The black bar represents the number of genes with an absolute value of $\log_2$ FC greater than 0.7, and the gray bar represents the number of genes with an absolute value of $\log_2$ FC less than 0.7. B) A heat map representing canonical pathway analysis (left panel). Activated canonical pathway (blue bar) and inhibited canonical pathway (red bar) were identified by applying absolute value of *Z* score > 2. FC value of selected DEGs that are related to the top three canonical pathways (right panel). C) Heat maps representing diseases and biological function analysis. Activated canonical pathway (blue bar) and inhibited canonical pathway (red bar) were identified by applying absolute value of *Z* score > 2. D, E) Comparison analysis of D) canonical pathways and E) diseases/bio functions between Treg-depleted and Treg-restored mice. *Z* scores were used to predict activation or inhibition. Statistical analyses were performed using the Wald test (*$P < 0.05$, compared with age-matched control mice, $n = 6$–9 mice for each group).

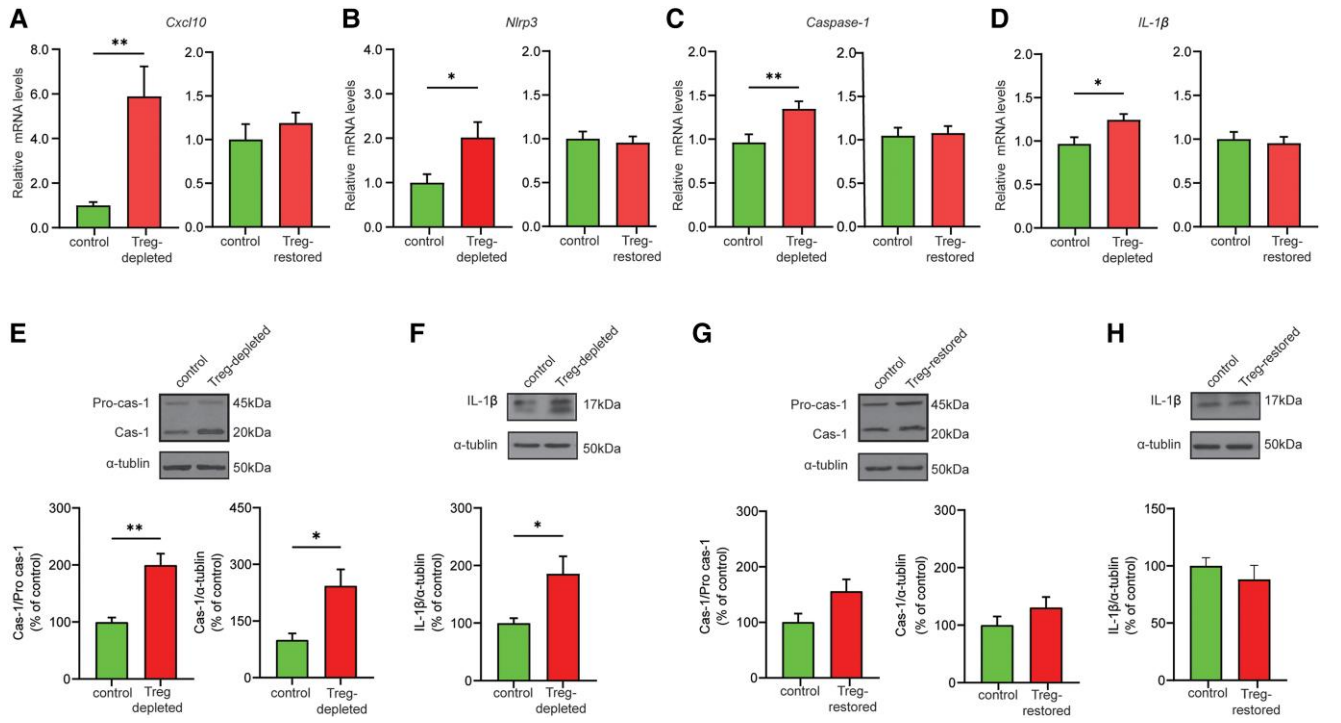

Fig. 4. Transient activation of inflammasome signaling pathway mediated by depletion of Foxp3-expressing cells in hippocampal formation of DEREG mice. A–D) The mRNA expression of Cxcl10, Caspase-1, Nlrp3, and IL-1β in hippocampal formation of Treg-depleted mice (left panels) and Treg-restored mice (right panels). Bar graphs showing relative quantification of Cxcl10 A), Caspase-1 B), Nlrp3 C), and IL-1β D) levels normalized Hprt. E–H) Representative western blot of Pro-casepase-1, Caspase-1, and IL-1β in Treg-depleted E, F) and Treg-restored mice G, H). Bar graphs showing relative quantification of cleaved Caspase-1, ratio Caspase-1/Pro-caspase-1 E, G), and IL-1β F, H) levels normalized α-tubulin. Statistical analyses were performed using *t* test (*$P < 0.05$, **$P < 0.01$, compared with age-matched control mice, $n = 4$–8 mice for each group). Data are expressed as the means ± SEM.

differences between Foxp3-depleted mice and age-matched control mice with respect to the percentage of $CD3e^{-}CD19^{+}$ cells, $CD3e^{+}CD19^{-}$ cells, $CD3e^{+}CD4^{+}$ cells, and $CD3e^{+}CD8^{+}$ cells (Fig. 5E and F). Interestingly, the percentage of $CD3^{-}CD19^{-}CD11b^{+}LY\text{-}6G^{+}$ cells (granulocytes, Fig. 5D, left panel) and $CD3^{-}CD19^{-}CD11b^{+}LY\text{-}6G^{-}$ cells (macrophages/monocytes, Fig. 5D, right panel) were significantly higher by 84 and 23%, respectively, compared with age-matched control mice (Fig. 5D).

Based on this evidence suggesting a role of Tregs in the regulation of innate immune cells, next we explored alteration of cytokines or chemokine production released by innate immune cells in plasma of Treg-depleted mice using a proteome profiler array. A total of six cytokines were altered in Treg-depleted mice with significantly four cytokines up-regulated (interferon-gamma [IFN-γ], macrophage-colony stimulating factor [M-CSF], triggering receptor expressed on myeloid cells-1 [TREM-1], and IL-13), one cytokine down-regulated (tissue inhibitor of metallopeptidase-1 [TIMP-1]), and a tendency toward one cytokine up-regulated (IL-17) compared with age-matched control mice (Fig. 5G). These results suggest the potential alteration of peripheral innate immunity through depletion of Foxp3-expressing cells.

Several studies have reported that granulocyte-derived MMP-9 activity may lead to damage of the BBB (27). Based on this evidence and our immune profiling outcome showing elevated levels of granulocyte and monocytes/macrophages, we continued to explore MMP-9 expression in the brain. As shown in Fig. 5H, Treg-depleted mice showed significant transient elevation of MMP-9 expression in the hippocampal formation (Fig. 5H) compared with age-matched control mice that we found being restored to baseline level in Treg-restored mice (Fig. 5I). These results suggest that depletion of Foxp3-expressing cells in PBMC may lead to an increase of innate immune cells, possibly influencing transient MMP-9 expression in the brain.

Depletion of Foxp3-expressing cells induces inflammasome activation coinciding with cognitive impairment and Aβ peptide burden in the hippocampal formation in the 5xFAD mice

Further IPA-derived functional network mapping analysis was performed to identify direct and indirect relationships among DEGs and DEGs' regulators in Treg-depleted mice, which suggested the "Developmental disorder, hereditary disorder, and metabolic disease" network being highly predicated among 31 molecules (score 48). Among them, we found amyloid precursor protein (APP) that is associated with pathogenesis of AD being predicted as a key molecule in Treg-depleted mice (Fig. 6A). To examine the relevance of this mechanism in AD pathogenesis, we generated a double transgenic 5xFAD/DEREG mouse model to investigate whether depletion of Foxp3-expressing cells in 5xFAD mice would alter behavior changes including anxiety- and depression-like behaviors, cognitive impairment, and AD neuropathology compared with 5xFAD mice (Fig. 6B). No observable alterations in anxiety- and depression-like behaviors were found in both the control and 5xFAD mice (Fig. 6C and D). Interestingly, after depletion of Foxp3-expressing cells, the 5xFAD mice exhibited a significant increase in the time spent in the dark area, indicative of increased anxiety-like behavior compared with 5xFAD (Fig. 6C). Additionally, we observed an increased immobility time, suggestive of depression-like behavior in 5xFAD/Treg-depleted mice compared with 5xFAD (Fig. 6D). We observed no significant differences in anxiety- or depression-like

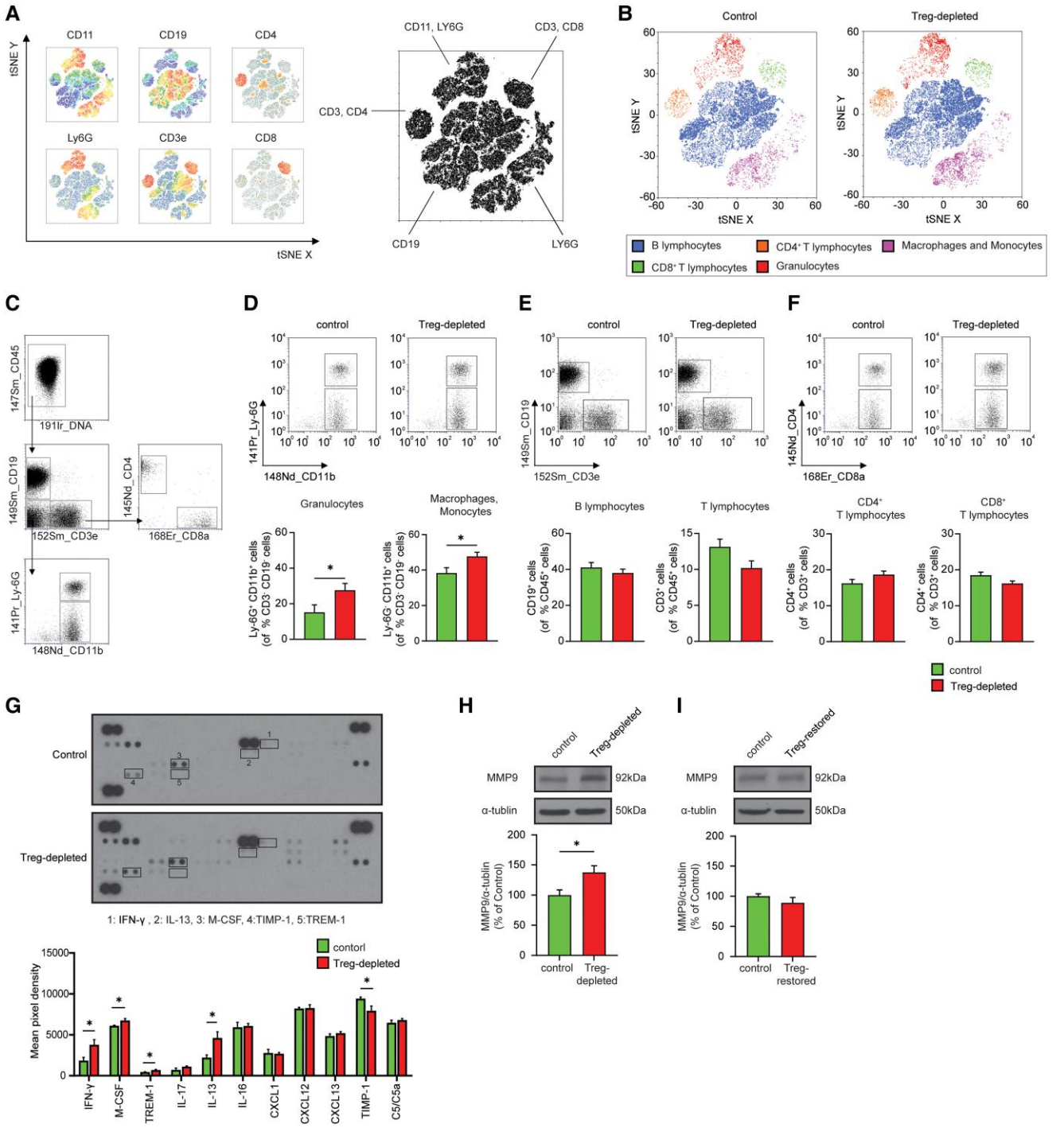

Fig. 5. Characterization of peripheral immune cell population and transient MMP-9 expression mediated by depletion of Foxp3-expressing cells in DEREG mice. A, B) t-SNE plots generated from the CD45$^+$ immune cell populations stained by CyTOF in PBMC of Treg-depleted mice. A) Heat maps showing expression of selected markers by immune cells clustered using t-SNE analysis. B) t-SNE plots separated into five broad groups of immune cells (B lymphocytes, CD4$^+$ T lymphocytes, CD8$^+$ T lymphocytes, macrophages/monocytes, and granulocytes) in Treg-depleted mice compared with age-matched control mice. The main cell populations are shown by the indicated color profile. C) Gating strategy for CyTOF analysis. D–F) Representative CyTOF scatter plots (upper panel) and quantification of lymphocyte subpopulation (bottom panel). Bar graphs showing percentage of CD11b$^+$LY-6G$^+$ D), CD11b$^+$LY-6G$^-$ D), CD3e$^-$ CD19$^+$ E, left panel), CD3e$^+$CD19$^-$ E, right panel), CD3e$^+$CD4$^+$ F, left panel), and CD3e$^+$CD8$^+$ F, right panel) cells in Treg-depleted mice compared with age-matched control mice. Scales are shown in biexponential scale. G) Representative blot image of the cytokine array data in Treg-depleted and age-matched control mice (upper panel). Bar graphs showing quantification of mean pixel density of cytokines and chemokines among 40 cytokines (bottom panel). The mean pixel densities of each spot were normalized by reference spots. H, I) Representative western blot of MMP-9 (upper panel). Bar graphs (bottom panel) showing relative quantification of MMP-9 level normalized α-tubulin in hippocampal formation of Treg-depleted mice H) and Treg-restored mice I). Statistical analyses were performed using *t* test. (*$P < 0.05$, compare with age-matched control mice, $n = 6$–8 mice for each group). Data are expressed as the means ± SEM.

behaviors between Treg-depleted mice and 5xFAD/Treg-depleted mice (Fig. 6C and D). This supports the hypothesis that the altered anxiety- and depression-like behaviors observed in 5xFAD/Treg-depleted mice are not driven by the genetic susceptibility in 5xFAD mice. Moreover, we found no significant change of locomotion activity between all experimental mice groups (Fig. 6E, bottom left panel). Interestingly, discrimination index as a measure of cognitive function significantly decreased in 5.5-month-old 5xFAD/Treg-depleted mice that are presymptomatic at this age as assessed by NOR (Fig. 6E, bottom right panel).

We next evaluated the levels of Aβ peptide and Aβ burden, the hallmark neuropathological characteristic of AD, assessed by ELISA and immunohistochemistry, respectively. We found statistical significance for reduction of $A\beta_{1–40}$ isoform and increase of $A\beta_{1–42}$ isoform, with resulting increase of $A\beta_{1–42}$/$A\beta_{1–40}$ ratio in hippocampal formation of 5xFAD/Treg-depleted mice (Fig. 6F). In addition, elevation of Aβ plaque burden was observed in dentate gyrus layer of hippocampal formation in 5xFAD/Treg-depleted mice compared with age-matched 5xFAD mice as assessed by 6E10 immunostaining (Fig. 6G).

This evidence was of high interests in view of the fact that inflammasome activation is currently implicated in mechanisms associated with Aβ pathology and neurodegeneration (28, 29). Based on this, we next examined the potential role of caspase-1 activation and IL-1β generation in 5xFAD/Treg-depleted mice (Fig. 6H and I). We found the protein expression of the active form of Caspase-1 in the hippocampal formation was significantly increased in 5xFAD/Treg-depleted mice compared with age-matched 5xFAD mice (Fig. 6H). In addition, 5xFAD/Treg-depleted mice showed an increasing trend of elevation of IL-1β compared with age-matched 5xFAD mice ($P = 0.0611$, Fig. 6I).

Taken together, these results demonstrate that depletion of Foxp3-expressing cells may lead to inflammasome activation, AD-type neuropathology, and acceleration of the onset of cognitive impairment in 5xFAD mice.

Discussion

In this study, we elucidate the potential role of Foxp3-expressing cells in the mechanism associated with neurobehavioral changes including anxiety- and depression-like behaviors using DEREG mice. Our study revealed that Foxp3 is a novel key factor in anxiety- and depression-like behaviors through dynamic regulation of inflammatory responses including increased in the number of innate immune cells in PBMC, BBB disruption, and inflammasome activation in the brain. Interestingly, all were restored into baseline level concomitantly with neurobehavioral recovery following restoration of Foxp3-expressing cells in DEREG mice.

Impaired function of Tregs has been implicated in the development of anxiety and depression (18, 19, 30, 31), and antidepressant/anxiolytic treatments are improved by increasing the number of Tregs and improving their function (32, 33). Our data demonstrate that transient anxiety- and depression-like behaviors were observed in DEREG mice, followed by DT treatment and then withdrawal of DT treatment to induce acute inflammation mediated by depletion of Foxp3-expressing cells and to return to its normal state through restoration of Foxp3-expressing cells, respectively. Our results are consistent with other studies that reported a potential relationship between Foxp3 and the development of anxiety- and depression-like behaviors. Interestingly, we found that both anxiety- and depression-like behaviors were significantly modulated dependent on Foxp3-expressing cells in PBMC (Fig. 2). Despite a distinct association between Foxp3 and anxiety-/depression-like behaviors, a detailed mechanism for peripheral and central immune communication in anxiety and depression has not yet been investigated.

Inflammasomes are composed of three components, including a cytosolic sensor protein such as NOD-, LRR-, and pyrin domain–containing protein 3 (NLRP3), an adaptor protein known as apoptosis-associated speck-like protein containing a caspase recruitment domain (ASC), and inflammatory caspases such as caspase-1 (34). The process of inflammasome formation and activation involves two steps: priming and activation (35). The priming signal is initiated by cytokines or damage-associated molecular patterns/pathogen-associated molecular patterns (DAMPs/PAMPs) recognized by receptors such as Toll-like receptors (TLRs), leading to the transcription, translation, and production of various genes including NLRP3, pro-IL-1β, and pro-caspase-1 (35). Subsequently, following a second activation signal induced by diverse stress signals, the assembly of the inflammasome is triggered, leading to the activation of caspase-1 and subsequent cleavage of pro-IL-1β into its mature form, IL-1β protein (35). A study reported that a chronic stress mouse model showed elevated NLRP3 inflammasome activation and IL-1β level in hippocampal formation associated with depression-like behavior (36). Inhibition of inflammasome activation in this model blocked depression-like behavior with reduced IL-1β production (36). In addition, mice lacking NLRP3 were resistant to anxiety-like behavior, and blockade of inflammasome activation signaling using P2X7 antagonist attenuated anxiety-like behavior (37, 38). Our results show that Treg-depleted mice showed inflammasome activation including increased cleavage of Caspase-1 and IL-1β production in hippocampal formation. Interestingly, we found that restoration of Foxp3-expressing cells ameliorated cleavage of Caspase-1 and IL-1β production in hippocampal formation concomitantly to neurobehavioral recovery (Figs. 3 and 4).

Elevated proinflammatory responses in the blood of MDD patients are closely linked to a higher prevalence of MDD, highlighting the significant association between heightened inflammatory state and an increased susceptibility and severity of mood disorders, including depression and anxiety (39–41). To examine the pathways and mechanisms underlying inflammasome activation in the brain, we hypothesized that activation of peripheral immune cells mediated by depletion of Foxp3-expressing cells may promote inflammasome activation through increased infiltration of innate immune cells into the brain. Our data demonstrate that the number of circulating innate immune cells, including granulocytes, is elevated and there is increased expression of proinflammatory cytokines, including IFN-γ, M-CSF, TREM-1, and IL-17, released from innate immune cells in Treg-depleted mice (Fig. 5). In addition, our data showed elevated expression of MMP-9 released by granulocytes, diminished TIMP-1 expression, a tissue inhibitor of metalloproteinase, and increased expression of *Cxcl10*, secreted by activated innate immune cells (Figs. 4 and 5). We also identified that the biological process associated with DEGs in Treg-depleted mice is “Immune cell trafficking” through IPA functional analysis (Fig. 3). Taken all together, our study suggests that activation of innate immune cells in peripheral may bridge the gap between inflammasome activation in brain and transient of Foxp3-expressing cells in PBMC, which is a key factor in the pathogenesis of anxiety- and depression-like behaviors.

Increased inflammatory processes in the peripheral can initiate neuroinflammation through diverse immune-to-brain signaling

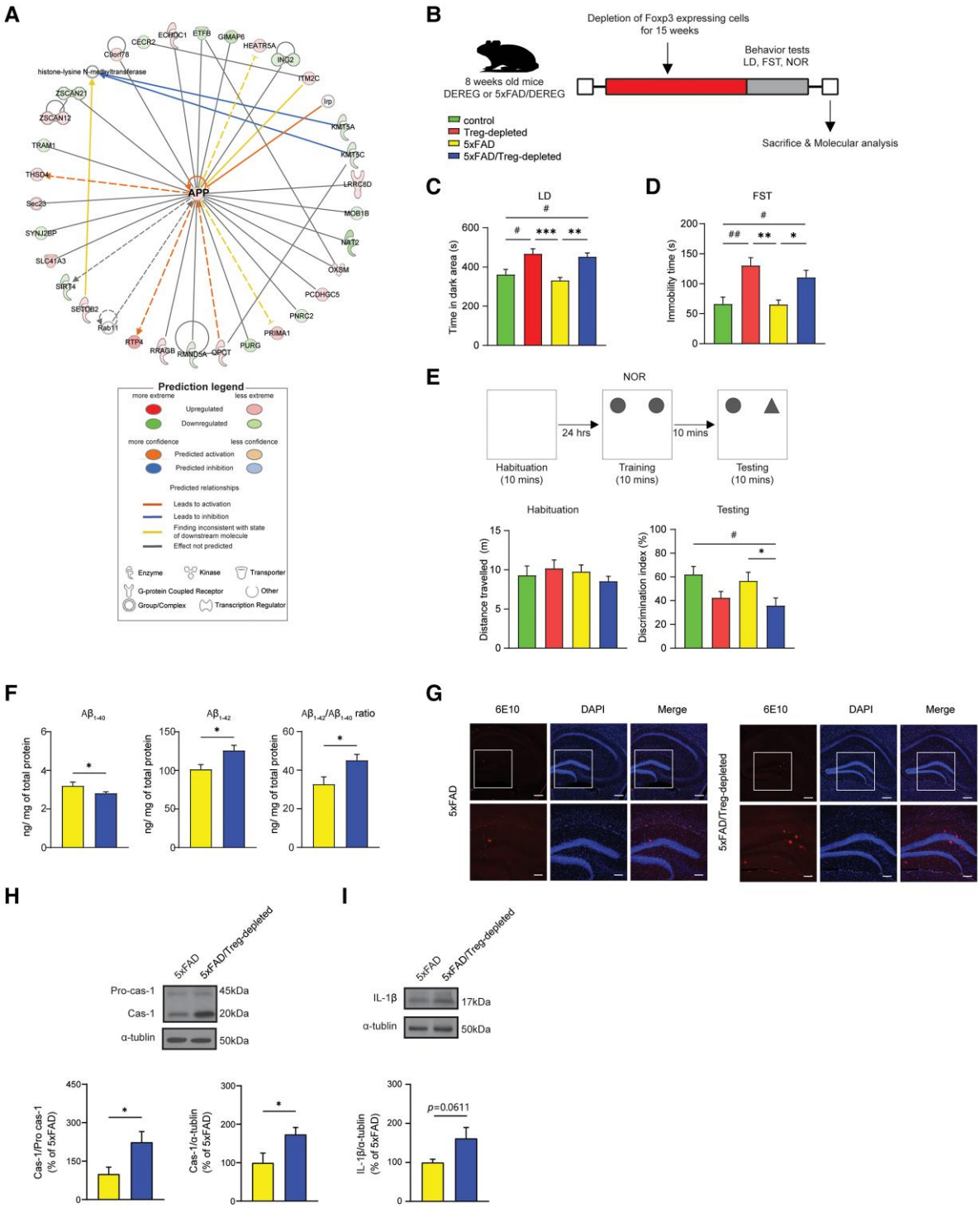

Fig. 6. Cognitive decline, accumulation of Aβ, and inflammasome activation mediated by depletion of Foxp3-expressing cells in 5xFAD/Treg-depleted mice. A) Functional gene networks identified using IPA analysis in hippocampal formation of Treg-depleted mice. Predict legend indicates each node's relationship from machine-based learning. B) Experimental outline (LD, light and dark box; FST, forced swimming test; NOR, novel objective recognition test) in control, Treg-depleted, 5xFAD, and 5xFAD/Treg-depleted mice. C) Bar graphs showing time spent in the dark compartment as a measure of anxiety-like behavior in LD. D) Bar graphs showing total immobility time compartment as measure of depression-like behavior in FST. E) Scheme illustration of NOR for the assessment of cognitive function (upper panel). Bar graphs showing locomotion activity as measure of total distance traveled in habituation session (bottom, left panel) and discrimination index as measure of percent time spend with the novel object in testing session (bottom, right panel). F) The level of soluble $A\beta_{1-40}$ and $A\beta_{1-42}$ in the hippocampal of 5xFAD/Treg-depleted mice. Bar graphs showing quantification of $A\beta_{1-40}$, $A\beta_{1-42}$, and the ratio of $A\beta_{1-42}/A\beta_{1-40}$ compared with age-matched 5xFAD mice. G) Representative immunohistochemical images showing 6E10-labeling Aβ plaques (red) and DAPI (blue) nuclei in the dentate gyrus of 5xFAD/Treg-depleted and age-matched 5xFAD mice. The outlined with a white box in the upper panel is magnified in the bottom panel. The scale bars indicate 200 μm (low-scaled panel) and 100 μm (magnified panel). H, I) Representative western blot of Pro-casepase-1, Caspase-1, and IL-1β in 5xFAD/Treg-depleted mice. Bar graphs showing relative quantification of cleaved Caspase-1 H, left panel), ratio of Caspase-1/Pro-caspase-1 H, right panel), and quantification of IL-1β I) levels normalized α-tubulin. Data are expressed as the means ± SEM. Statistical analyses were performed using t test or two-way ANOVA, followed by Tukey's post hoc analysis ($^{*}P < 0.05$, $^{**}P < 0.01$, $^{***}P < 0.001$ compared with age-matched 5xFAD control mice; $^{\#}P < 0.05$, $^{\#\#}P < 0.01$ compared with age-matched DEREG control mice, $n = 6$–10 mice for each group).

pathways, involving the transport of cytokines or chemokines across BBB to gain entry into the brain when the BBB is compromised or absent (42). Moreover, the binding of these cytokines or chemokines, functioning as DAMPs/PAMPs, to specific receptors such as TLRs on microglia, triggers the activation of inflammasomes in MDD (43). In line with these findings, our study supports that pharmacological intervention promoting Foxp3-expressing cells in PBMC may causally attenuate acute forms of anxiety- and depression-like behaviors coincidentally with restoration of potentially innate immune-mediated cascades in the brain. We hypothesize that chronic inflammatory responses mediated by depletion of Foxp3-expressing cells eventually cause irreversible neurological damages including BBB disruption and a permissive proinflammatory state, leading to chronic inflammation in the brain explaining certain forms of untreatable anxiety and depression conditions. Further studies are needed to investigate the potential role of chronic depletion of Foxp3-expressing cells in anxiety- and depression-like behaviors associated with risk of irreversible brain degeneration including permeant BBB damage. Our study provides evidence that the depletion of Foxp3-expressing cells is causally linked to the emergence of transient anxiety- and depression-like behaviors, which are associated with immune system plasticity. Importantly, our additional behavior tests and biochemical experiments conducted on wild type mice, with vehicle and DT treatment, revealed no significant changes of body weight, neurobehavioral changes, and inflammasome activation in the brain (Fig. S1). These findings suggest that any observed effects on altered neurobehavioral and immune response are specifically associated with the depletion of Foxp3-expressing cells rather than the influence of DT treatment itself.

Depression and anxiety are observed in the early stage of AD patients with cognitive decline (44, 45). The prevalence of anxiety ranges from 9.4 to 39%, and the prevalence of depression ranges from 14.8 to 40% in various stages of AD (46). In addition, recent studies revealed a significant strong relationship between anxiety, depression, cognitive decline, and neuropathology of AD (47). Similarly, we found that depletion of Foxp3-expressing cells induced inflammasome activation, influencing AD-like neuropathological changes and exacerbating cognitive impairment at a presymptomatic stage in 5xFAD mice (Fig. 6). Multiple evidence have confirmed that NLRP3 inflammasome plays a causal role in pathogenesis of AD (48). For examples, the oligomer and fibrillar forms of Aβ provide the priming signal, as a kind of DAMPs, which are recognized by TLRs for NLRP3 inflammasome activation (49, 50). This indicates that the innate immune response in the brain may occur prior to the deposition of Aβ plaques. Indeed, recent studies have provided evidence from cell experiments and animal models, demonstrating that inflammasome-dependent formation of ASC specks can also impact the deposition and spread of Aβ, potentially influencing the onset or progression of AD (51). The activation of the NLRP3 inflammasome is mediated through two main types of signaling pathways (52). The first is the canonical signaling pathway, which is related to the recruitment of pro-caspase-1 and subsequent activation of caspase-1 (52). The second is the noncanonical signaling pathway, mainly associated with the activation of mouse caspase-11 or human caspase-4 and caspase-5 (52). Despite the extensive research on NLRP3 inflammasome activation induced by several factors has been extensively studied in AD, there is still a need for further exploration of the exact molecular mechanisms involved. Particularly, limited knowledge is available regarding the noncanonical pathway in AD. Based on our study, Foxp3-driven inflammasome pathway may play an important role in the onset and progression of AD. Further in-depth studies are needed to validate potential mechanisms related to innate and adaptive immunity alteration in peripheral and central immune system to elucidate specific molecular mechanisms mediated by Foxp3-expressing cells in AD. Moreover, our findings suggest that modulating central immune responses mediated by Foxp3-expressing cells in the peripheral system could be a potential therapeutic strategy in AD. However, further investigations are necessary to assess the feasibility and effectiveness of targeting the Foxp3-driven inflammasome pathway as a therapeutic intervention for AD. Additional research is needed to evaluate the potential benefits and drawbacks of modulating this pathway, which will provide valuable insights for the development of future therapeutic approaches for AD.

Collectively, our study supports that Foxp3 may causally influence peripheral immune response that induces transient proinflammatory cascade in the brain, leading to anxiety- and depression-like behaviors or cognitive decline.

Acknowledgments

This manuscript was posted on a preprint (https://doi.org/10.21203/rs.3.rs-2410197/v1). G.M.P. holds a Senior VA Career Scientist Award. We acknowledge that the contents of this study do not represent the views of the U.S. Department of Veterans Affairs, the NCCIH, the ODS, the National Institutes of Health, or the United States Government. The authors would also like to thank Joshua Palmieri for his impeccable work with administrative duties.

Supplementary material

Supplementary material is available at *PNAS Nexus* online.

Funding

Research reported in this publication was supported by the National Center For Complementary & Integrative Health of the National Institutes of Health under Award Number U19AT010835. The content is solely the responsibility of the authors and does not necessarily represent the official views of the National Institutes of Health. This research was supported by a grant (BX0005054) from the U.S. Department of Veterans Affairs (VA) awarded to G.M.P.

Author contributions

E.-J.Y. conceived and designed the study concept, performed all experiments, analyzed and interpreted the data, and was instrumental in the writing of the manuscript. E.G. conducted the research and analyzed the data. R.I.-A. and M.A.R. contributed to performing the research. G.M.P. conceived and designed the study concept and supervised the project. In addition, G.M.P. is the guarantor of this work, as such; he has full access to all the data in the study and takes responsibility for the integrity of the data and the accuracy of the data analysis. All authors read the final version of the manuscript, revised it critically, and gave final approval of the version submitted.

Data availability

All data are included in the manuscript and/or supporting information.

References

1 Gold SM, *et al.* 2020. Comorbid depression in medical diseases. *Nat Rev Dis Primers*. 6:69.
2 Duman RS, Aghajanian GK, Sanacora G, Krystal JH. 2016. Synaptic plasticity and depression: new insights from stress and rapid-acting antidepressants. *Nat Med*. 22:238–249.
3 Wohleb ES. 2016. Neuron-microglia interactions in mental health disorders: "for better, and for worse". *Front Immunol*. 7:544.
4 Afridi R, Suk K. 2021. Neuroinflammatory basis of depression: learning from experimental models. *Front Cell Neurosci*. 15: 691067.
5 Beumer W, *et al.* 2012. The immune theory of psychiatric diseases: a key role for activated microglia and circulating monocytes. *J Leukoc Biol*. 92:959–975.
6 Wohleb ES, Franklin T, Iwata M, Duman RS. 2016. Integrating neuroimmune systems in the neurobiology of depression. *Nat Rev Neurosci*. 17:497–511.
7 Hodes GE, Kana V, Menard C, Merad M, Russo SJ. 2015. Neuroimmune mechanisms of depression. *Nat Neurosci*. 18: 1386–1393.
8 Miller AH, Raison CL. 2016. The role of inflammation in depression: from evolutionary imperative to modern treatment target. *Nat Rev Immunol*. 16:22–34.
9 Engelhardt B, Vajkoczy P, Weller RO. 2017. The movers and shapers in immune privilege of the CNS. *Nat Immunol*. 18: 123–131.
10 Luissint AC, Artus C, Glacial F, Ganeshamoorthy K, Couraud PO. 2012. Tight junctions at the blood brain barrier: physiological architecture and disease-associated dysregulation. *Fluids Barriers CNS*. 9:23.
11 Prinz M, Priller J. 2017. The role of peripheral immune cells in the CNS in steady state and disease. *Nat Neurosci*. 20:136–144.
12 Sun Y, Koyama Y, Shimada S. 2022. Inflammation from peripheral organs to the brain: how does systemic inflammation cause neuroinflammation? *Front Aging Neurosci*. 14:903455.
13 Lee W, Lee GR. 2018. Transcriptional regulation and development of regulatory T cells. *Exp Mol Med*. 50:e456.
14 Ramsdell F, Ziegler SF. 2014. FOXP3 and scurfy: how it all began. *Nat Rev Immunol*. 14:343–349.
15 Hayatsu N, *et al.* 2017. Analyses of a mutant Foxp3 allele reveal BATF as a critical transcription factor in the differentiation and accumulation of tissue regulatory T cells. *Immunity* 47: 268–283.e9.
16 Lucca LE, Dominguez-Villar M. 2020. Modulation of regulatory T cell function and stability by co-inhibitory receptors. *Nat Rev Immunol*. 20:680–693.
17 Dominguez-Villar M, Hafler DA. 2018. Regulatory T cells in autoimmune disease. *Nat Immunol*. 19:665–673.
18 Grosse L, *et al.* 2016. Deficiencies of the T and natural killer cell system in major depressive disorder: T regulatory cell defects are associated with inflammatory monocyte activation. *Brain Behav Immun*. 54:38–44.
19 Toben C, Baune BT. 2015. An act of balance between adaptive and maladaptive immunity in depression: a role for T lymphocytes. *J Neuroimmune Pharmacol*. 10:595–609.
20 Prelog M, *et al.* 2016. Hypermethylation of FOXP3 promoter and premature aging of the immune system in female patients with panic disorder? *PLoS One*. 11:e0157930.
21 Jahangard L, Behzad M. 2020. Diminished functional properties of T regulatory cells in major depressive disorder: the influence of selective serotonin reuptake inhibitor. *J Neuroimmunol*. 344:577250.
22 Leger M, *et al.* 2013. Object recognition test in mice. *Nat Protoc*. 8: 2531–2537.
23 Westfall S, *et al.* 2021. Chronic stress-induced depression and anxiety priming modulated by gut-brain-axis immunity. *Front Immunol*. 12:670500.
24 Yang EJ, *et al.* 2021. Modulation of neuroinflammation by low-dose radiation therapy in an animal model of Alzheimer's disease. *Int J Radiat Oncol Biol Phys*. 111:658–670.
25 Okeke EB, Uzonna JE. 2019. The pivotal role of regulatory T cells in the regulation of innate immune cells. *Front Immunol*. 10:680.
26 Romano M, Fanelli G, Albany CJ, Giganti G, Lombardi G. 2019. Past, present, and future of regulatory T cell therapy in transplantation and autoimmunity. *Front Immunol*. 10:43.
27 Galea I. 2021. The blood-brain barrier in systemic infection and inflammation. *Cell Mol Immunol*. 18:2489–2501.
28 Heneka MT, *et al.* 2013. NLRP3 is activated in Alzheimer's disease and contributes to pathology in APP/PS1 mice. *Nature* 493:674–678.
29 Ising C, *et al.* 2019. NLRP3 inflammasome activation drives tau pathology. *Nature* 575:669–673.
30 Grosse L, *et al.* 2016. Circulating cytotoxic T cells and natural killer cells as potential predictors for antidepressant response in melancholic depression. Restoration of T regulatory cell populations after antidepressant therapy. *Psychopharmacology (Berl)*. 233: 1679–1688.
31 Chen Y, *et al.* 2011. Emerging tendency towards autoimmune process in major depressive patients: a novel insight from Th17 cells. *Psychiatry Res*. 188:224–230.
32 Schneider-Schaulies J, Beyersdorf N. 2018. CD4+ Foxp3+ regulatory T cell-mediated immunomodulation by anti-depressants inhibiting acid sphingomyelinase. *Biol Chem*. 399:1175–1182.
33 Singh A, *et al.* 2020. Anxiolytic drug FGIN-1-27 ameliorates autoimmunity by metabolic reprogramming of pathogenic Th17 cells. *Sci Rep*. 10:3766.
34 Broz P, Dixit VM. 2016. Inflammasomes: mechanism of assembly, regulation and signalling. *Nat Rev Immunol*. 16:407–420.
35 Guo H, Callaway JB, Ting JP. 2015. Inflammasomes: mechanism of action, role in disease, and therapeutics. *Nat Med*. 21: 677–687.
36 Zhang Y, *et al.* 2015. NLRP3 inflammasome mediates chronic mild stress-induced depression in mice via neuroinflammation. *Int J Neuropsychopharmacol*. 18:pyv006.
37 Alcocer-Gomez E, *et al.* 2016. Stress-induced depressive behaviors require a functional NLRP3 inflammasome. *Mol Neurobiol*. 53:4874–4882.
38 Iwata M, *et al.* 2016. Psychological stress activates the inflammasome via release of adenosine triphosphate and stimulation of the purinergic type 2X7 receptor. *Biol Psychiatry*. 80:12–22.
39 Xia CY, *et al.* 2023. The NLRP3 inflammasome in depression: potential mechanisms and therapies. *Pharmacol Res*. 187: 106625.
40 Fleshner M, Frank M, Maier SF. 2017. Danger signals and inflammasomes: stress-evoked sterile inflammation in mood disorders. *Neuropsychopharmacology* 42:36–45.
41 Iwata M, Ota KT, Duman RS. 2013. The inflammasome: pathways linking psychological stress, depression, and systemic illnesses. *Brain Behav Immun*. 31:105–114.
42 Capuron L, Miller AH. 2011. Immune system to brain signaling: neuropsychopharmacological implications. *Pharmacol Ther*. 130: 226–238.
43 McCusker RH, Kelley KW. 2013. Immune-neural connections: how the immune system's response to infectious agents influences behavior. *J Exp Biol*. 216:84–98.

44 Lyketsos CG, *et al.* 2002. Prevalence of neuropsychiatric symptoms in dementia and mild cognitive impairment: results from the cardiovascular health study. *JAMA* 288: 1475–1483.
45 Botto R, Callai N, Cermelli A, Causarano L, Rainero I. 2022. Anxiety and depression in Alzheimer's disease: a systematic review of pathogenetic mechanisms and relation to cognitive decline. *Neurol Sci*. 43:4107–4124.
46 Ma L. 2020. Depression, anxiety, and apathy in mild cognitive impairment: current perspectives. *Front Aging Neurosci*. 12:9.
47 Pink A, *et al.* 2022. A longitudinal investigation of Aβ, anxiety, depression, and mild cognitive impairment. *Alzheimers Dement*. 18: 1824–1831.
48 Zhang Y, Dong Z, Song W. 2020. NLRP3 inflammasome as a novel therapeutic target for Alzheimer's disease. *Signal Transduct Target Ther*. 5:37.
49 Halle A, *et al.* 2008. The NALP3 inflammasome is involved in the innate immune response to amyloid-beta. *Nat Immunol*. 9:857–865.
50 Sita G, Graziosi A, Hrelia P, Morroni F. 2021. NLRP3 and infections: β-amyloid in inflammasome beyond neurodegeneration. *Int J Mol Sci*. 22:6984.
51 Friker LL, *et al.* 2020. β-amyloid clustering around ASC fibrils boosts its toxicity in microglia. *Cell Rep*. 30:3743–3754.e6.
52 Liang T, Zhang Y, Wu S, Chen Q, Wang L. 2022. The role of NLRP3 inflammasome in Alzheimer's disease and potential therapeutic targets. *Front Pharmacol*. 13:845185.